2010

On the Optimal Water Discharge Temperature of Air-to-Water Heat Pump for Space Heating and Domestic Hot Water

Noma Park
LG Electronics

Hyoung-Suk Woo
LG Electronics

Jong-Chul Ha
LG Electronics

Dong-Hyuk Lee
LG Electronics

Simon Chin
LG Electronics

On the Optimal Water Discharge Temperature of Air-to-Water Heat Pump for Space Heating and Domestic Hot Water

Noma PARK[1], Hyoung-Suk WOO[1], Jong-Chul HA[1], Dong-Hyuk LEE[1], and Simon CHIN[1]

[1]LG Electronics Inc., Corporate Air Conditioning R&D Laboratory
327-23, Gasan-Dong, Geumcheon-Gu, Seoul, 153-802, Korea
Phone: +82-55-260-3860, e-Mails: noma.park@lge.com, hyoungsuk.woo@lge.com, Jongchul.ha@lge.com, dhyuk.lee@lge.com, simon.chin@lge.com

* Corresponding Author

ABSTRACT

In the present study, optimal water discharge temperature of heat pump for radiator heating is investigated, which is one of the main issues of air-to-water heat pump as the formal replacement of gas- or oil-fired boiler. To this end, thermal characteristics of radiator are investigated to find temperature required to match thermal loads of considered reference site at Paris, France. It is shown that water discharge temperature up to 70^{o}C is required for the one-to-one replacement of current boilers. However, detailed numerical simulation showed that running heat pump at the same condition with boiler results in unacceptably low COP even with heat pump suited for high temperature. This issue is resolved by simple and novel water temperature control method, which results in the significant reduction in annual running cost and payback period.

1. INTRODUCTION

Recently in the EU countries, air-to-water heat pumps (AWHPs) are rapidly replacing conventional gas-fired or oil-fired boilers thanks to various subsidies for heat pumps in addition to their inherent energy saving and low CO2 emission properties. However, there are some unresolved issues for AWHPs to be the perfect replacement of boilers. One item that most concerns customers is the hot water discharge temperature. Unlike boilers whose discharge temperature is up to 80^{o}C, that of AWHP is usually around 50^{o}C when R410A is used as the refrigerant. In order to reduce this gap, there are currently three possible alternatives: the use of electric resistance sub-heater at higher temperature than specified value, the use of alternative refrigerant with higher condensing temperature such as R407C, and the use of a cascade system with two cycles installed.

However, even with these alternatives, running heat pumps at high discharge temperature is not always desirable in view of efficiency especially when the outdoor temperature is low. Thus, it is of crucial importance for heat pump manufacturers to estimate the optimal water discharge temperature that maximizes seasonal COP and, at the same time, perfectly matches the heating load. In this study, the optimal water discharge temperature of AWHP for space heating and domestic hot water (DHW) is investigated via numerical simulation and supporting experiments, in terms of efficiency and load matching capability.

Toward this end, one needs an accurate estimation of annual running cost of AWHP. In this study, such analysis is given by using detailed metrological data, domestic hot water usage pattern into an in-house simulation code that integrates AWHP cycle, radiator heating, and stratified hot water storage tank. The present paper is organized as follows: In Section 2, we describe the main characteristics of AWHP Considered in this study. Thermal characteristics of radiator are given in Section 3. Then, governing equation, numerical method, floor heating simulation method, outdoor temperature and hot water usage pattern are given in Section 4. Discussion of simulation results are given in Section 4, and the summary and conclusions are given in Section 6.

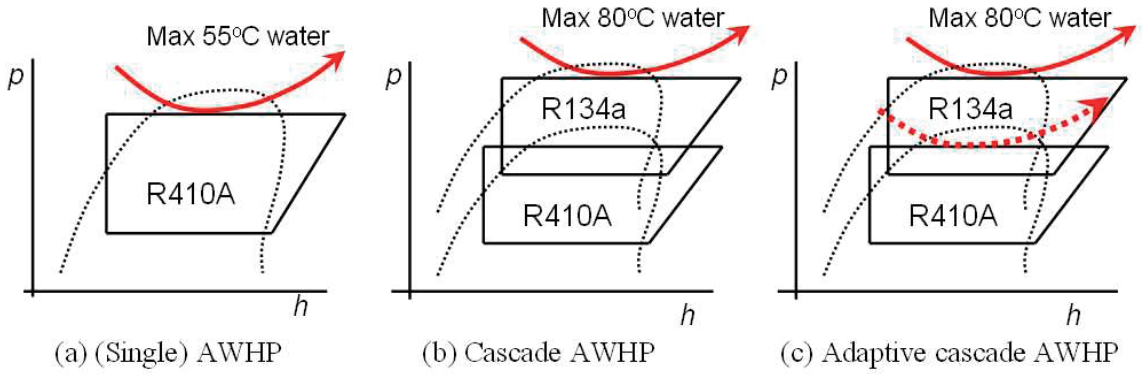

Figure 1: Mollier diagrams of air-to-water heat pumps: (a) single AWHP; (b) Cascade AWHP; (c) Adaptive cascade AWHP

2. AIR-TO-WATER HEAT PUMPS

Cycle diagrams for AWHPs considered in this study are summarized in Figure 1. Shown in Figure 1(a) is the first AWHP released in the market, which is the combination of general heat pump outdoor unit and a "hydro-kit" composed of a water-to-refrigerant heat exchanger (HEX), water pump and control box. It is assumed that its nominal capacity is 16kW and uses R410A as the refrigerant, and, thus, the maximum water discharge temperature is 55°C. Although it is possible to raise the temperature up to desired temperature by using electric heater, this option is not considered in this study.

A viable alternative to electric heater is introducing a cascade cycle with refrigerant such as R134a suitable for discharging high temperature water up to 80°C, whose p-h diagram is shown in Figure 1(b). Now, the hydro-kit is expanded to include internal refrigerant-to-refrigerant HEX, R134a compressor, expansion valve, together with water-to-refrigerant HEX pumps. In what follows, we will refer this system to 'cascade AWHP'. In contrast to this, R410A AWHP in Figure 1(a) is referred to as 'single AWHP'. A salient feature of cascade AWHP considered in this study is that inverter compressors are adopted for both R410A and R134a cycles so that heat pump can actively correspond to variable load conditions.

The main concern of cascade AWHP is the efficiency of partial load conditions with low pressure ratios, or low water discharge temperature. As will be shown later, in general, COP of cascade AWHP is lower than that of single AWHP when water temperature is lower than 40°C. Thus, in order to take the best of both system, a hybrid AWHP can be considered as shown in Figure 1(c): this system switches between single and cascade AWHP by using three-way valves for both water and refrigerant. However, one needs a separate condenser to realize this idea. Therefore, the main question is whether increased efficiency is worth an additional HEX. In what follows, this system is denoted as 'adaptive cascade'AWHP.

3. SPACE HEATING WITH RADIATOR

In this section, a numerical model for the radiator and water discharge temperature control method is proposed as the core part of the AWHP simulation.

3.1 Thermal model of radiator

As show in Figure 2, we consider thermal balance of the radiator based on column-by-column approach. For each column of the radiator, heat transferred to the room by a column is equivalent to heat loss by the temperature decrease across pipe:

$$\delta Q_i = h_{n,c} A\left(T_{s,i} - T_{amb}\right) + \sigma\varepsilon A\left(T_{s,i}^4 - T_{amb}^4\right) = -\dot{m} C_{p,w}\left(T_{i+1} - T_i\right), \quad (1)$$

where $T_{s,i}$ and $T_{s,i+1}$ denote averaged surface temperatures of the radiator columns with area A under consideration and its neighbor, respectively, and T_i and T_{i+1} are corresponding water temperatures flowing inside the pipe. Here, σ is the Stefan-Boltzmann constant, $\varepsilon = 0.8$ is the emissivity of radiation. By successively applying equation (8) to successive columns, one can determine the entire surface temperature distribution, total heat transferred to the room, and return water temperature. $h_{n,c} = k\overline{Nu_L}/L$ is the natural heat transfer coefficient determined by (Churchill and Chu 1975)

$$\overline{Nu}_L = \left\{0.825 + \frac{0.387 Ra_L^{1/6}}{[1 + (0.492/\mathrm{Pr})^{9/16}]^{8/27}}\right\}^2, \quad (2)$$

where Ra_L is the Rayleigh number, and $L = A/\wp$ is the characteristic length, and $\wp$ is the perimeter of the area segment. Inserting realistic parameters and 80°C water to (1) and (2) gives that overall heat transfer coefficient of the radiator is around 5~10 W/m^{2}K and heat capacity of one radiator amounts to approximately 1kW, which agrees well with data on vendor provided specification sheets.

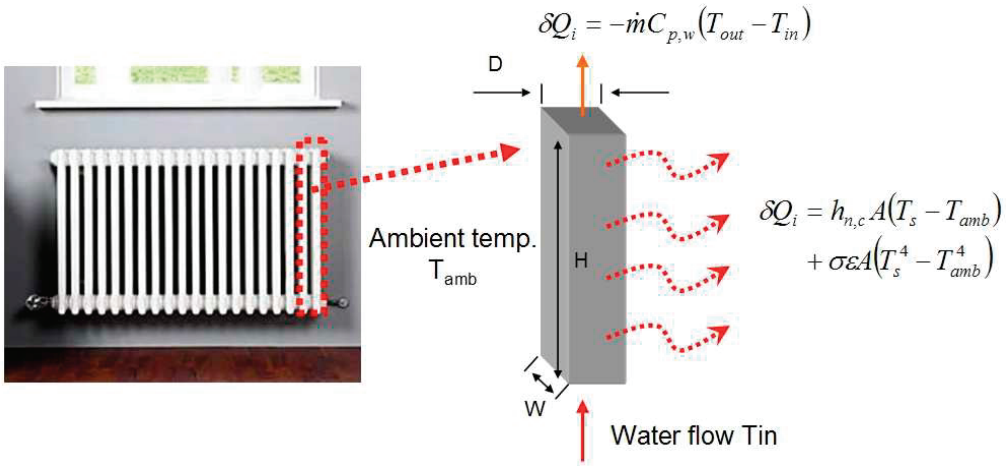

Figure 2: Numerical modeling of a radiator: thermal balance for a column.

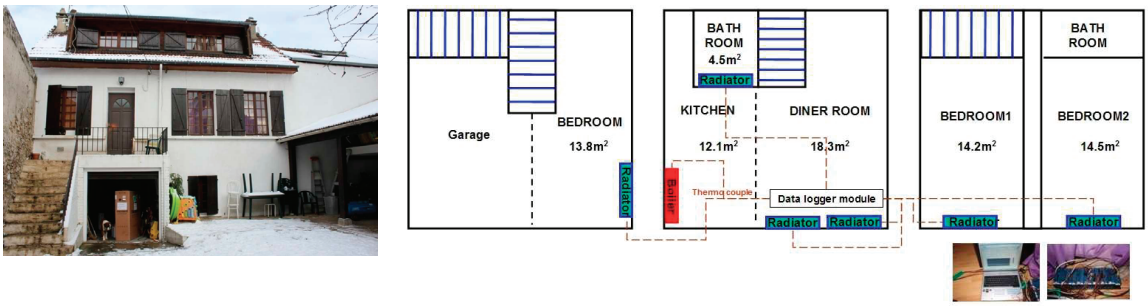

Figure 3: Field test house at Pontois, France and blueprint showing detailed heating space.

3.2 Dynamic water control scheme

The main objective of heating is to maintain desired indoor temperature with minimal deviation or fluctuation. To this end, heat pumps with fixed rotation frequency usually turn on and off compressors frequently. Whereas heat pumps adopting inverter accomplish this objective by changing the rotation frequency of the compressor according to given load. As will be shown later, desired heat pump capacity is

$$Q_{\text{ideal}} = h_{id} A_{house} (T - T_{\text{amb}}), \tag{3}$$

with which indoor temperature remains unchanged once it reaches setting value. However, imposing Q_{ideal} as target is impractical since the exact value of loss coefficient h is hard to know and is changing according to external weather condition. In practice, so called 'weather compensated control' is often adopted to achieve energy saving, which changes target discharge temperature to be prescribed on corresponding to outdoor temperature. However, there is no guarantee that prescribed target temperature is right one to match thermal load.

Here, we propose a dynamic discharge water temperature control method purely based on thermo off time, or time required to raise indoor temperature up to thermostat setting temperature. The main idea is to increase (reduce) discharge temperature when measured thermo-off time is too long (short) as compared to target thermo-off time. This method appears sound in the sense that ill-designed air conditioning devices with excessive capacity result in frequent thermo-off, and vice versa. The logical expression for this control is summarized as follows:

$$\begin{cases} if\ T_{thermo-off} > T_{target,\max} \rightarrow T_{set,new} = T_{set} + dT^{+}, \\ if\ T_{thermo-off} < T_{target,\min} \rightarrow T_{set,new} = T_{set} - dT^{-}, \\ if\ no\ thermo-off\ until\ T_{fail} \rightarrow T_{set,new} = 75^{o}C, \end{cases} \tag{4}$$

where $T_{\text{target,min}}$ and $T_{\text{target,max}}$ are, respectively, minimal and maximum allowable target thermo-off times. The last condition is the failsafe condition to prevent no thermo-off due to unexpected decrease of outdoor temperature, which is proven to be necessary. The temperature increment dT^{+} and dT^{-} are given by

$$\begin{aligned} dT^{+} &= \min\left(dT_{\max}, \frac{\left| T_{target,\max} - T_{thermo-off} \right|}{T_{target,\max}} dT_{\max} \right), \\ dT^{-} &= \min\left(dT_{\max}, \frac{\left| T_{target,\min} - T_{thermo-off} \right|}{T_{target,\min}} dT_{\max} \right), \end{aligned} \tag{5}$$

where a rather arbitrary value $dT_{\max} = 10^{o}\text{C}$ is set as the limitation of the increment to ensure mild variation of temperature. The main advantage of the current control is that it is completely black box approach, which does not need any other information than thermo-off time. Thus, it is applicable to any heating and cooling system compatible with discharge air/water temperature variation. The impact of the proposed control method on the energy efficiency will be investigated in the following section.

4. NUMERICAL SIMULATION

4.1 Reference site and measured data analysis

In order to obtain insight into the current boiler operation, field measurement at Pontois, suburban area of Paris, France was performed on December, 2009. The reference house selected is a 3 story single house with 64m^2 actual heating space, as shown in Figure 3. Heating device is a 24 kW gas-fired boiler, and terminal units are five radiators.

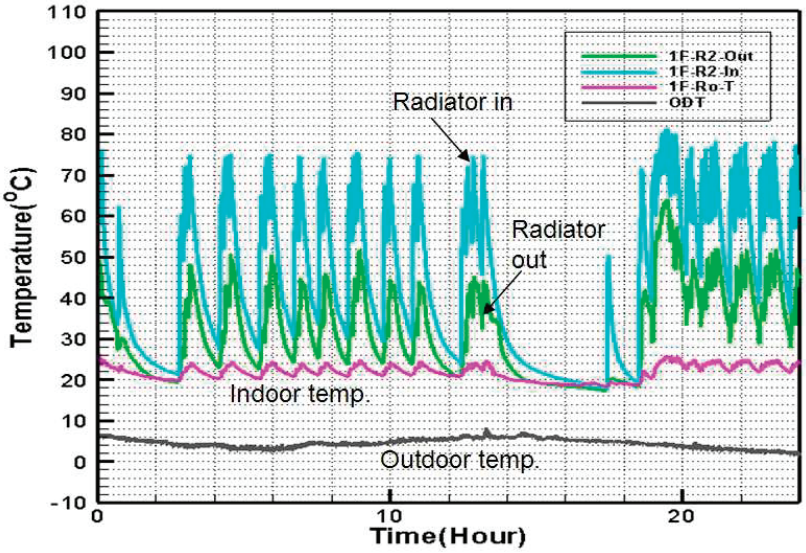

Figure 4: Instantaneous radiator input/output, indoor, and outdoor temperatures measured at the reference site

Figure 4 shows instantaneous temperature evolutions at radiator input, output, indoor, and outdoor during a day, which tells valuable information besides radiator inlet temperature is over 70°C. Since it was impossible to measure water flow rate, it is conjectured from temperature difference between radiator inlet and outlet by using equations (1) and (2) as follows: 1) from guessed mass flow rate, one can compute return water temperature. 2) If this value does not match measured temperature, iterate with a new guess until convergence is achieved. Water mass flow rate computed in this way is 4.5 LPM, and corresponding radiator heat is 6.5 kW when the indoor temperature is 20°C. Since measured inflow and return temperature drops across pipe, respectively, were 3°C and 2°C, total heat loss is about 2.4 kW and thus heat capacity by boiler is 8.9 kW. From the operation pattern shown in Figure 4, which shows frequent thermo on-off, we can conjecture that actual thermal load is much less than 6.5 kW.

In order to estimate thermal load and heat loss coefficient of the reference house, heat equation for the house is solved:

$$m_{id} C_{p,air} \frac{dT_{id}}{dt} = Q_{radiator} - h_{id} A_{house} (T_{id} - T_{od}), \tag{6}$$

where Q_{radiator} is the heat ejection from radiator computed by equations (1) and (2), T_{id} is the indoor temperature, m_{id} air mass in the house, h_{id} heat loss coefficient, A_{house} the surface area of the house, and T_{od} is the outdoor temperature. From measured data and temperature variation pattern, all values but h_{id} is known. Thus, it is readily computed as $h_{id} \approx 0.8 W/m^2 K$. Using this value, thermal load corresponding to given outdoor temperature can be determined, which is shown in Figure 5(a). Since the lowest outdoor temperature is -7°C in this area, this value is the design point of heat pumps. From Figure 5(a), thermal load is less than 5kW at this temperature. This explains the frequent thermo-off behavior of radiator at higher heat emission shown in Figure 4.

Also shown in Figure 5(b) is desired radiator inlet temperature to match thermal load at given water mass flow rate. It is shown that at design temperature water discharge temperature should be higher than 65°C at 4.5 LPM mass flow rate. It is reduced up to 57°C by increasing water mass flow rate. However, temperature drop by increasing mass flow rate is not significant since as is evident from equations (1) and (2), absolute temperature determines heat ejected by the radiator.

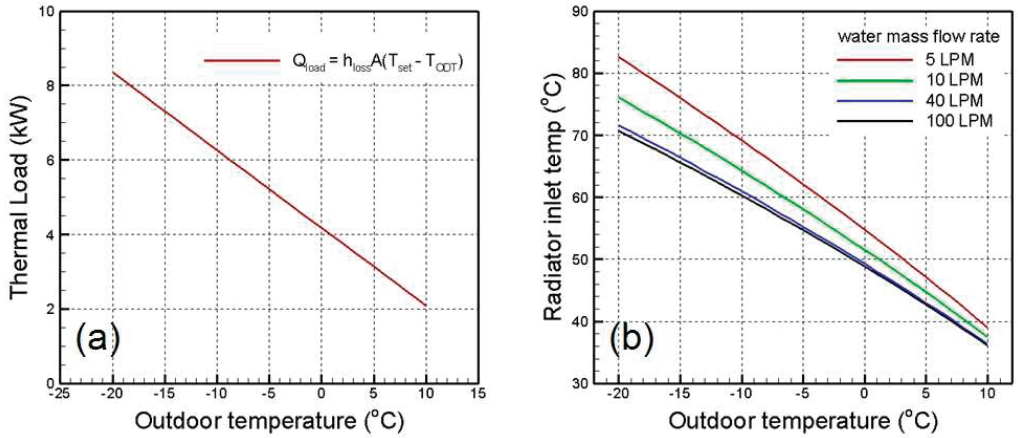

Figure 5: Relationship between outdoor temperature and radiator inlet water for the reference house at Pontois, France: (a) Thermal load corresponding to outdoor temperature and (b) radiator inlet water temperature required to match thermal load.

From above analysis, single AWHP appears not to be an appropriate solution for the reference site, whose discharge temperature cannot exceed 55°C. Thus, in what follows, we will focus on cascade and adaptive cascade AWHPs.

4.2 Governing equations

As shown in Figure 6, we consider a simplified model house with 8m (L) by 8m (D) by 2.7m (H) size, and a 0.5m diameter, 200 liter sanitary tank. In order to simplify the simulation single zone is considered. However, this approach can be easily expanded to multi-zone simulation. The main purpose of this simulation is to run heat pumps to maintain setting indoor and sanitary tank temperature as actual heating system does, and to measure corresponding energy consumption.

Indoor temperature is given by equation (6), where radiator capacity is determined by the following one-dimensional unsteady heat equation for closed loop pipe system:

$$\rho_w C_{p,w} A_{pipe}\left(\frac{\partial T_{loop}}{\partial t} + u\frac{\partial T_{loop}}{\partial s}\right) = -q_{radiator}(s) + q_{hp}(s) + kA_{pipe}\frac{\partial^2 T_{ST}}{\partial s^2} - h_{pipe}\wp\left(T_{loop} - T_{od}\right), \quad (7)$$

where T_{loop} is temperature through closed loop water pipe, and $q_{radiator}(s)$ is one-dimensional profile of radiator heat whose value satisfy $\int q_{radiator}(s)ds = Q_{radiator}$, A_{pipe} and $\wp$ are the surface area and perimeter of pipe, respectively, and s is the coordinate along the closed loop. $q_{hp}(z)$ denotes heat capacity given by heat pump. Similarly, sanitary tank temperature are assumed to obey the following one-dimensional energy equation

$$\rho_w C_{p,w} A_{ST}\left(\frac{\partial T_{ST}}{\partial t} + u\frac{\partial T_{ST}}{\partial z}\right) = q_{hp}(z) + kA_{ST}\frac{\partial^2 T_{ST}}{\partial z^2} - h_{ST}\wp\left(T_{ST} - T_{id}\right), \quad (8)$$

Where T_{id} and T_{ST} are, respectively, temperatures of indoor and sanitary tank, and z denotes coordinate direction of tank height. Here, A_{ST} the cross sectional area of sanitary tank, and $\wp$ the perimeter of the sanitary tank. The loss coefficients h_{pipe} and h_{ST} are given as h_{pipe} = 7 W/m^{2}K, and h_{ST} = 0.83 W/m^{2}K. h_{pipe} is computed from heat loss measured at the reference site and h_{ST} is from the measurement data at the laboratory.

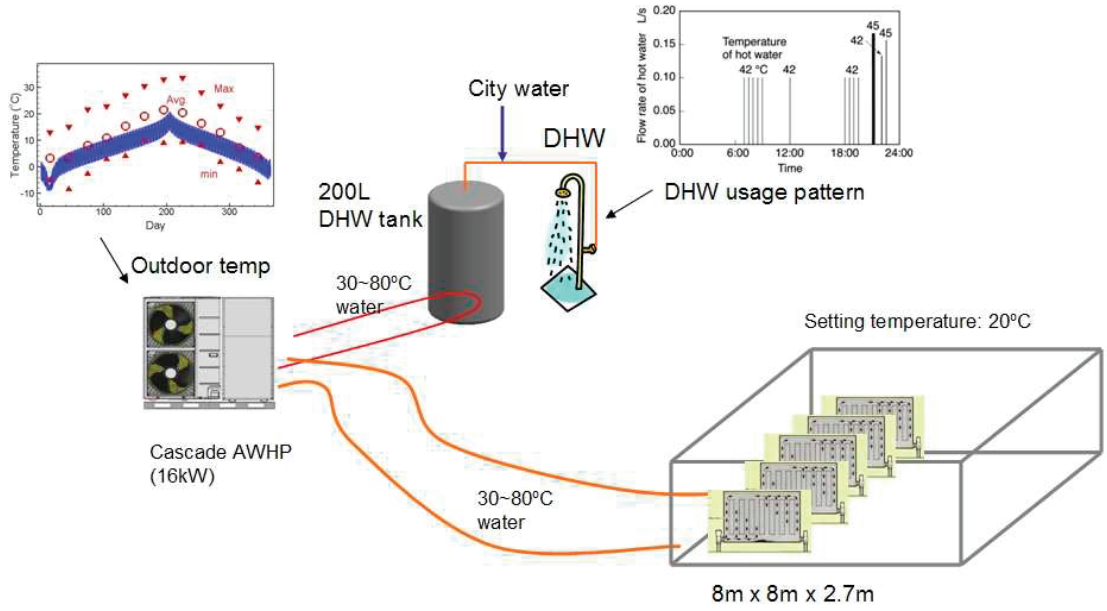

Figure 6: Schematics on numerical simulation for annual running cost estimation of heat pump.

Since energy consumption by DHW takes relatively small portion in the total energy consumption, equation (8) can be replaced by a lumped one like equation (6) without causing significant error. However, one-dimensional system is preferred to accurately see the effect of stratification on the energy consumption. For the spatial discretization of (7) and (8), third-order upwind difference and second order central difference are adopted for convection and diffusion terms, respectively. For the temporal integration of (1) and (2), 4th order Runge-Kutta method is applied at fixed time step $\Delta t = 1$ sec, and the integration is carried out for a year, or for $365 \times 24 \times 3600 = 31{,}536{,}000$ time steps.

A special care should be given to the boundary conditions of equation (8), since the inlet and outlet mixing has significant impact on the temperature distribution. We followed the definition of mixing parameter derived by Nelsol *et al.* (1998) for boundary conditions. The validation of stratified sanitary tank model against experiment is given in Figure 7: in order to see mixing effect at inlet and discharge, only tapping hot water without reheating is considered, through a hole located near the uppermost part of the tank. Initial averaged temperature is 50^{o}C and tapping flow rate is 4.8 LPM, and city water at 15^{o}C is entering into the bottom part of the sanitary tank at the same mass flow rate. As shown in Figure 7, the agreement with experimental data is acceptable.

4.3 Weather and DHW usage pattern

In order to integrate equations (6) and (7), one needs outdoor temperature data and daily hot water consumption amount and detailed usage pattern. For outdoor temperature, we created hourly temperature variation based on available monthly mean outdoor temperature data of Paris, and temperature bin (or PDF) data at Pontois, Paris. Figure 8 compares generated outdoor temperature with measured monthly mean data and bin data to see reasonable agreement especially with bin data.

For daily hot water usage pattern, we adopt a standard JRA data for DHW (Yokoyama *et al.* 2010) as shown in Figure 9. Change of daily DHW usage is modeled by multiplying constant factors to the pattern shown in Figure 9. In this study, 200 liter of daily hot water consumption is assumed throughout a year.

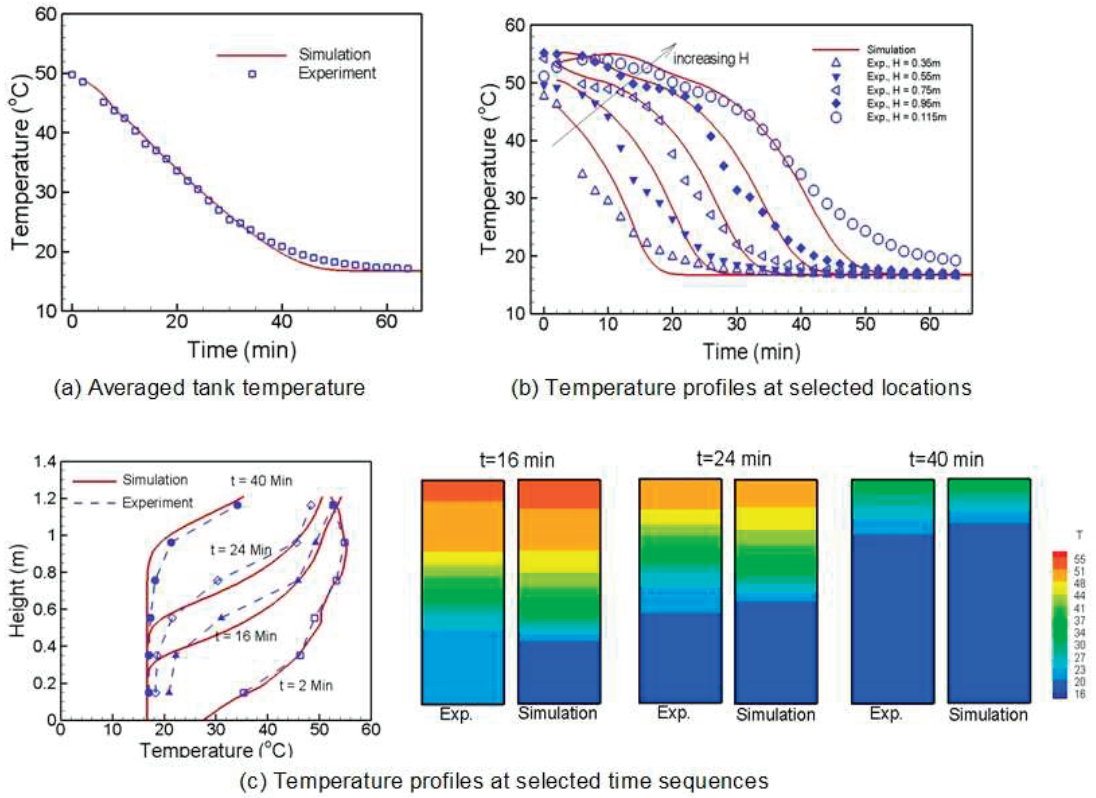

Figure 7: Validation of stratified sanitary tank model under tapping condition

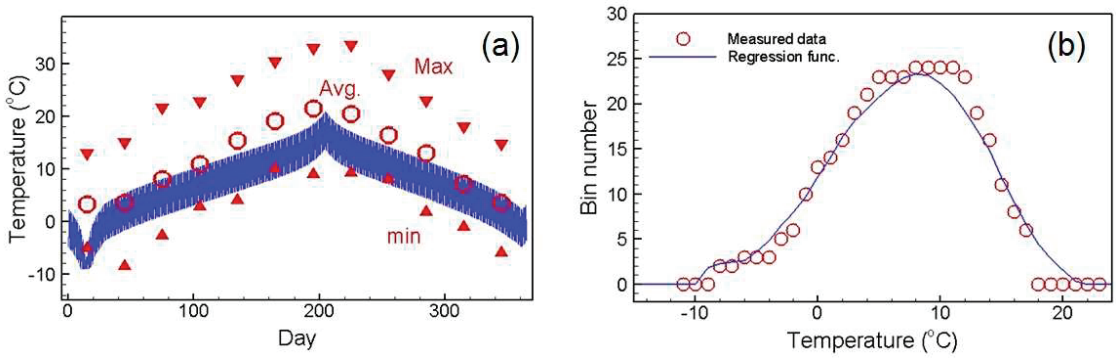

Figure 8: Weather data at Pontois, France: (a) temporal evolution of outdoor temperature; (b) temperature bin data

4.4 Calculation of energy consumption

Since inverter compressor is adopted heating capacities are subject to change according to thermal loads through the control logic described earlier. In order to compute required power input for given heat capacity and outdoor/indoor conditions, one can numerically simulate heat pump based on models on compressor, evaporator, condenser and expansion devices (see, e.g. Zhao *et al*. 2003). However, such a detailed numerical simulation is not appropriate for the present annual running cost simulation due to significant computational overhead. Instead, we have plenty of laboratory data measured at various outdoor temperature, water temperature and load conditions. By using these data, the coefficient of performance (COP) of AWHP is given by

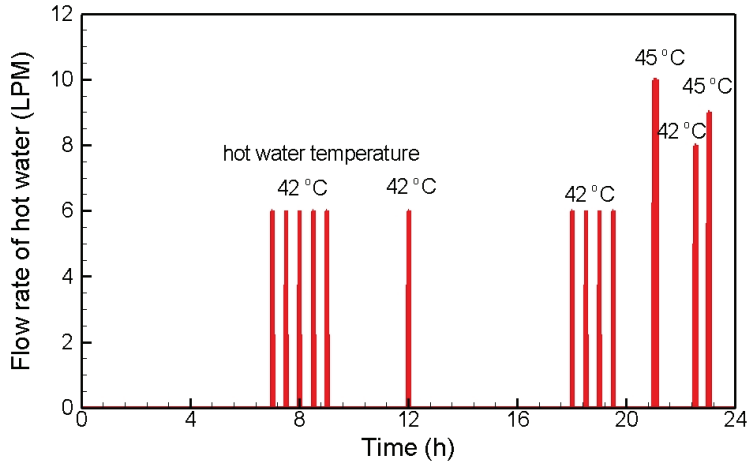

Figure 9: Model of daily DHW consumption pattern

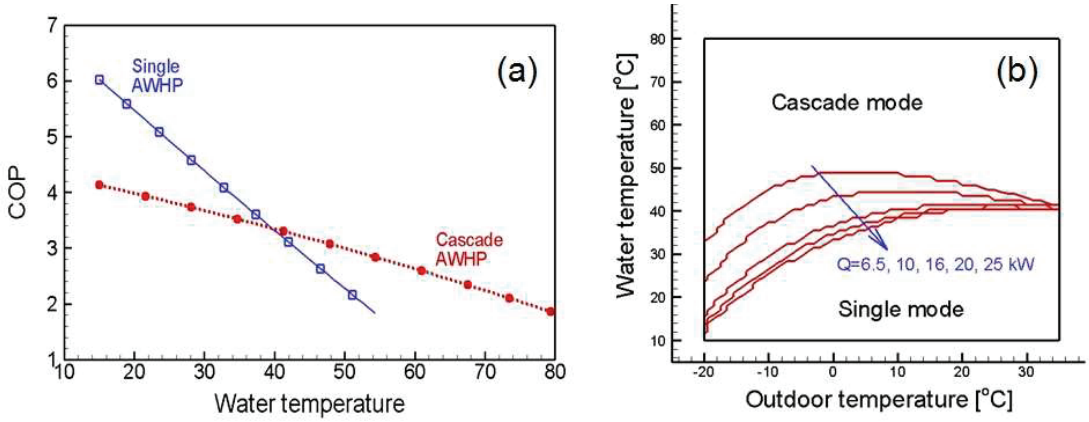

Figure 10: COP of AWHP: (a) COP vs. water inlet temperature at 7oC outdoor temperature and nominal heat pump capacity of 16 kW; (b) Single-cascade switch criteria for adaptive cascade AWHP at various outdoor temperatures, water temperatures and load conditions.

$$COP = h_0 + h_1 T_w + h_2 T_w^2 + h_3 T_{od} + h_4 T_{od}^2 + h_5 Q + h_6 Q^2 + h_7 T_w T_{od} + h_8 T_w Q + h_9 T_{od} Q, \quad (9)$$

where coefficients $h_0 \sim h_9$ are determined from the least-square fit of experimental data. Figure 10 compares COPs of single and cascade AWHP at 7°C outdoor temperature and 16kW heat capacity, which given by equation (9) with different coefficients sets. It is shown that COP of single AWHP is higher than that of cascade AWHP when water temperature is lower than 40°C, while cascade is the only solution for water temperature above it. Thus, we can make switch criteria for given outdoor temperature, water temperature and heat pump capacity, which is shown in Figure 10(b). It is shown that the area covered by single AWHP, or the region where single AWHP is more efficient, becomes wider as the heat pump load decreases. Thus, it would be interesting to see how much saving in energy consumption is achieved by using adaptive cascade AWHP. over cascade AWHP.

Once we know heating capacity and corresponding COP the energy consumption during a specified period is readily computed by

Table 1: Summary of annual simulation

	Gas-fired boiler	Cascade (Fixed temperature)	Cascade (Dynamic temperature)	Adaptive Cascade (Dynamic temperature)
Efficiency (COP)	0.85	2.33 (SCOP)	3.21 (SCOP)	3.87 (SCOP)
Initial Cost (Euro)	5,500	9,450	9,450	10,278
Fuel/Elec. cost	0.06 Euro/kWh	0.1183 Euro/kWh	0.1183 Euro/kWh	0.1183 Euro/kWh
Yearly energy consumption	15,561 kWh (DHW 3,682 kWh; heating 11,879 kWh)	5,705 kWh (DHW 1,137 kWh; heating 4,568 kWh)	3,836 kWh (DHW 1,137 kWh; heating 2,699 kWh)	3,184 kWh (DHW 1,137 kWh; heating 2,047 kWh)
CO_2 creation	3,143 kg/year	2,681 kg/year	1,803 kg/year	1,497 kg/year
Energy bill (Euro)	934	675	454	377
Payback period	-	15.3 yrs	8.2 yrs	8.5 yrs

$$E_{heating}(t_1 \sim t_2) = \int_{t_1}^{t_2} \frac{Q_{heating}}{COP_{heating}} dt. \tag{10}$$

Energy consumption by cooling and DHW can be computed in the same way.

5. RESULTS AND DISCUSSION

Results from annual simulation of AWHP are summarized in Table 1, where overall COP, yearly energy consumption, CO2 creation, are energy cost are listed. Initial cost in Table 1 is the summation of the product price and installation cost. For the case of AWHPs, 25% of subsidy for the product is applied. Assuming that we are to replace the current boiler installed at the reference site with AWHP, we can readily compute payback period based on the running cost and initial cost.
For cascade with fixed discharge water temperature at 75°C, seasonal COP (SCOP) from this simulation is only 2.33 and thus payback period is longer than 15 years, meaning that this is not the solution. Here, SCOP means the ratio between yearly summation of heat delivered over the summation of power input. This low COP issue is almost resolved by dynamic water temperature control to yield significantly enhanced SCOP of 3.21. Using dynamic water temperature control we can expect 480 Euro saving of annual energy cost, and corresponding payback period is 8.2 years. The efficiency is further enhanced by adaptive cascade yielding SCOP of 3.87. With adaptive cascade AWHP, annual saving of energy cost over boiler is 557 Euro, and corresponding payback is 8.5 years. Therefore, in view of life time cycle cost, adaptive cascade is most competitive. While, this result demonstrates that cascade AWHP is also competitive as far as efficient water temperature control logic is present.

In order to see the impact of dynamic water temperature control method on instantaneous thermal behavior, temperatures at indoor, outdoor, sanitary tank, radiator inlet, and radiator outlet are plotted in Figure 11 for fixed water temperature control and dynamic one on march 20, an arbitrary date. It is no wonder that current AWHP at fixed water temperature simulation shows a striking similarity of thermal behavior of boiler shown in Figure 4, since it is the one-to-one replacement of gas boiler at the same water mass flow rate and water discharge temperature. On the one hand, it is nice to see that heat pump can replace boiler without modification thanks to cascade cycle technology. On the other hand, however, the present result clearly shows that one cannot expect high enough COP to guarantee a timely payback with this one-to-one replacement. As shown in Figure 11(b), a simple change of discharge temperature control logic significantly reduces discharge water temperature, while indoor temperature is exactly at desired target value of 20°C within 1°C deviation.

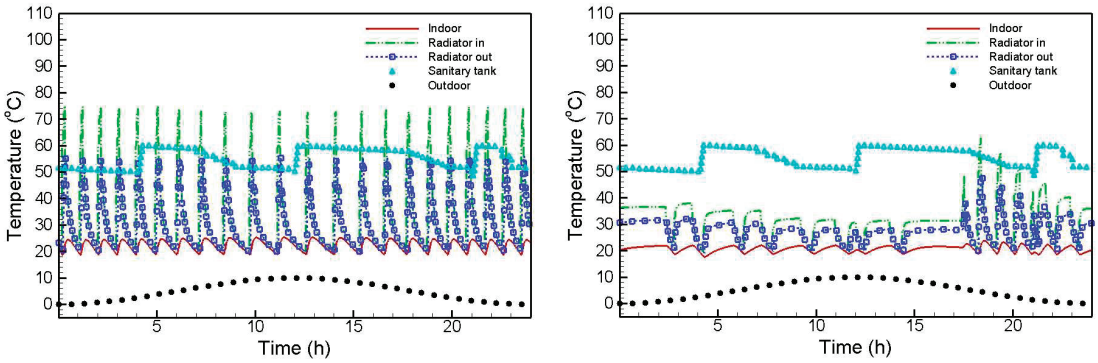

(a) Fixed water discharge temperature (b) Dynamic water discharge temperature

Figure 11: Instantaneous indoor, radiator, and outdoor temperatures on March 20 from numerical simulation with fixed and dynamic water temperature control method

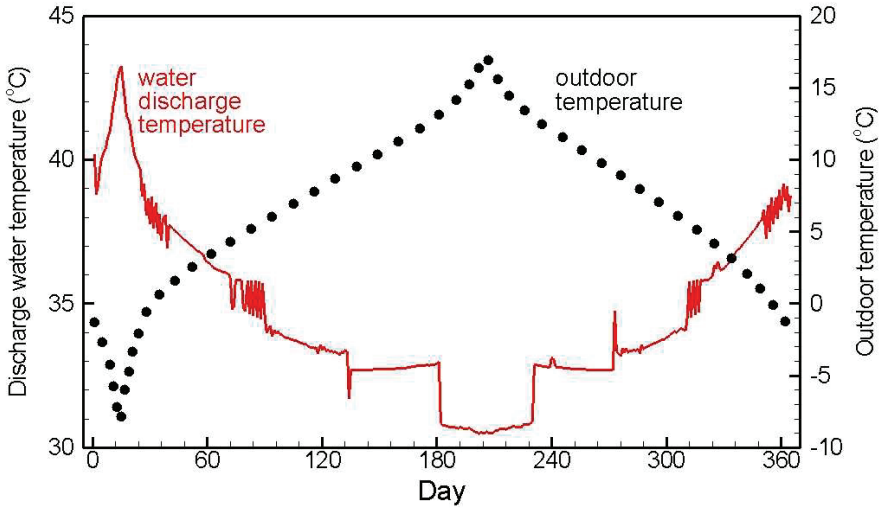

Figure 12: Daily mean outdoor and discharged water temperatures

It is seen that total 14 thermo-off events occurred during a day, which corresponds to 103 minute average thermo-off time. This means that the current dynamic control with 120 minute target thermo-off time is successfully working. Here $T_{target,min}$ and $T_{target,max}$ are set 90 and 150 minutes, respectively. It is interesting to see at near 6PM, discharge temperature rises up to 70°C to compensate excessive thermo-off time at near 3PM due to decreased outdoor temperature. Therefore, the capability of discharging high temperature water is used, but only for a short period when high water temperature is absolutely needed.

In order to the optimality of current dynamic temperature control method, daily mean outdoor and discharged water temperatures are shown in Figure 12. It is clear that mean discharged temperature shows a strong correlation with outdoor temperature, and this implies that the current method is a nice weather compensated control, although it is a black-box method which does not need outdoor temperature information. Figure 13 shows PDF of discharged water temperature and corresponding heat pump capacity from the current annual simulation with dynamic water control. It is shown that most operation occur near 35°C and 3kW capacity during a year, which implies that enhancement of heat pump efficiency at partial load condition at low compressor frequency is required, and that adaptive cascade cycle is definitely beneficial.

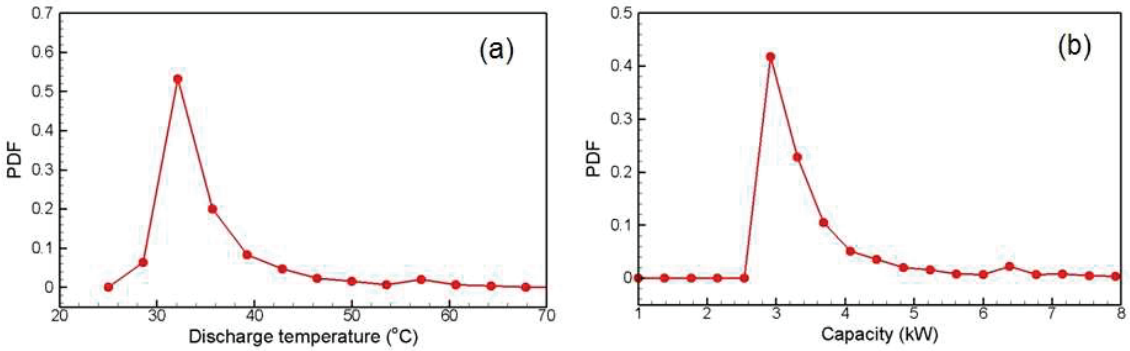

Figure 13: PDF of (a) discharge water temperature and (b) corresponding heat pump capacity from annual simulation of (adaptive) cascade AWHP.

So far we have focused on space heating. Actually, DHW significantly influences the annual energy consumption since COP for DHW is in general lower than space heating. Thus, by using current annual simulation, the optimal setting temperature of sanitary tank and the optimal heat pump capacity is evaluated. To this end, we use two different measures: The first one is the annual energy consumption for DHW defined as equation (10). The second one is annual RMS temperature deviation from indoor target temperature

$$T_{dev} = \sqrt{\frac{1}{T}\int_0^T (T_{id} - T_{set})^2 dt}. \qquad (11)$$

T_{dev} is very important since DHW and heating does not occur simultaneously, which means that heating should be stopped when DHW is on and vice versa. Figure 14(a) shows T_{dev} and energy consumption as the function of sanitary tank setting temperature. Here, the lowest setting temperature is 48°C, below which heat pump is exclusively working to raise sanitary tank temperature until setting temperature is reached. As shown when setting temperature is too low, heat pump should work on DHW more frequently so that space heating becomes less satisfactory. It appears that there is the optimum temperature in terms of Tdev, since at high setting temperature it takes too much time for heat pump to raise tank temperature, which is the case shown in Figure 14(b) with setting temperature of 75°C. At near 9PM, heat pump works exclusively on raising tank temperature so that indoor temperature drops to 16°C. Whereas, in terms of energy consumption, low setting temperature is better since heat pump COP is higher at lower temperatures. Considering both measures, setting temperature around 55°C ~ 65°C seems to be the best choice.

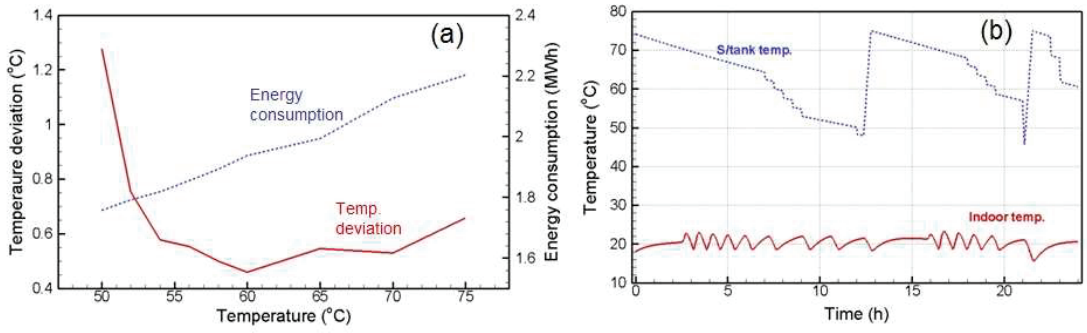

Figure 14: Optimal setting temperature of DHW for maximum energy saving and minimal temperature deviation. (a) RMS temperature deviation from setting indoor target and annual energy consumption for DHW; (b) Instantaneous temperature evolution when setting temperature is 75°C. Here, the lowest setting temperature of DHW is fixed at 48°C, and 300 liter of daily DHW consumption is assumed.

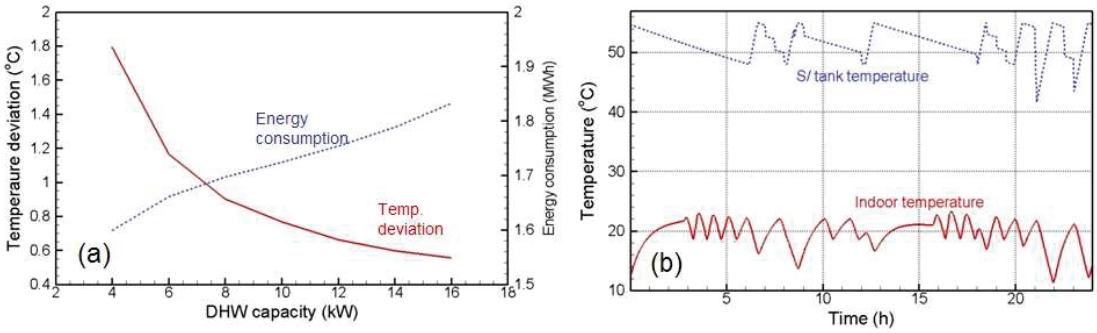

Figure 15: Optimal heat pump capacity of DHW for maximum energy saving and minimal temperature deviation. (a) RMS temperature deviation from setting indoor target and annual energy consumption for DHW; (b) Instantaneous temperature evolution when heat pump capacity is 4kW.

Finally, optimal heat pump capacity is estimated using the same measures mentioned above. If we consider minimization of T_{dev}, it is absolutely beneficial to use high capacity for DHW to reach target temperature as fast as possible and then heat pump can focus on space heating for the rest of time. This conjecture is actually true as shown in Figure 15. On the other hand, energy consumption is inversely proportional to the capacity as shown in Figure 15(b). Thus, the optimum should be the compromise between comfortable heating and low energy cost. However, since RMS temperature fluctuation should be less than 1^{o}C, heat pump capacity should be higher than 8kW: as shown in Figure 15(b) low capacity for DHW results in failure of space heating. Therefore, the use of DHW can be a compelling reason of using high nominal capacity heat pump, which is far higher than actual thermal load.

6. CONCLUSIONS

In the present study, the optimal water discharge temperature of heat pump for radiator heating was investigated, which is one of the main issues of air-to-water heat pump as the formal replacement of gas- or oil-fired boiler. To this end, thermal characteristics of radiator were investigated to find temperature required to match thermal loads of considered reference site at Paris, France.

It was shown that water discharge temperature up to 70 degree is required for the one-to-one replacement of current boilers. However, detailed numerical simulation showed that running heat pump at the same condition with boiler results in unacceptably low COP even with heat pump suited for high temperature. This issue was resolved by simple and novel water temperature control logic, which shows significant running cost reduction is achieved.

However, it should be noted that the current results are based on data measured at a specific reference site. The generalization of the idea requires consideration of several factors, which are water mass flow rate, the insulation property of building material, the number of radiator, the amount of hot water used, and the size of the sanitary tank. Since we have established general numerical models, the investigation into these effects can be readily done, and is the topic of our subsequent research.

REFERENCES

Churchill, S. W., and Chu, H. H. S., 1975, Correlating equations for laminar and turbulent free convection from a vertical plate, *Int. J. Heat Mass Transfer*, vol. 18: pp. 1323 - 1332.

Nelsol, J. E. B., Balakrishnan, A. R., Srinivasa Murthy, S., 1998, Transient analysis of energy storage in a thermally stratified water tank, *Int. J Ener. Res.*, vol. 22: p 867 – 883.

Yokoyama, R., Wakui, T., Kamakari, J., Takemura, K., 2010, Performance analysis of a CO2 heat pump water heating system under a daily change in a standardized demand, *Energy*, vol. 35: pp. 718-728.

Zhao, P.C., Ding, G. L., Zhang, C. L., Zhao, L., 2003, Simulation of a geothermal heat pump with non-azeotropic mixture, *Applied Thermal Engineering* 23: p 1515–1524.

ACKNOWLEDGEMENT

This work was supported by Air Conditioning Research and Development Laboratory in LG Electronics Inc.